

nary and $a+d = \pm 2$ the cut off conditions will be obtained. The cut off may be either between loss and phase shift as in a Zobel filter or between gain and phase shift because the cosine is an even function; therefore, it cannot perceive if the hyperbolic transformation is due to gain (negative resistance) or loss.

If the impedance plane is mapped onto the Riemann sphere, the criterion for determining whether the network is in the stop or pass band will depend on whether the Pascal line⁵ cuts or does not cut the Riemann sphere (the parabolic transformation occurs at tangency). These transformation characteristics have been used by Bolinder⁶ to show the analogy of the exponential line to the high pass filter and can be used to denote the difference between lossy and lossless uniform transmission lines. This classification can be used for any device, as waveguide, which has cut off phenomena or accounts for losses in any transmission device.

Thus it is seen that it is always possible to find reference terminals for a given network at which the resultant is either pure gain or pure loss or pure phase shift in the Zobel sense. Of course the insertion loss will depend on the termination as well as the properties of the two port.

D. J. R. STOCK

L. J. KAPLAN

Elec. Engrg. Dept.
New York Univ., N. Y.

⁵ E. F. Bolinder, "Impedance transformations by extension of the isometric circle method to the three dimensional hyperbolic space," *J. Math. Phys.*, vol. 36, pp. 49-61; April, 1957.

⁶ E. F. Bolinder, "Study of the exponential line by the isometric circle method and hyperbolic geometry," *Acta Pol.*, Elec. Engrg. Series, vol. 7, no. 8; 1957.

Characteristic Impedance of Split Coaxial Line*

A few years ago, the balun was studied at our laboratory and it is important to know the characteristic impedances of the line. There are several papers¹⁻³ concerning this characteristic impedance. The cross section of the transmission lines is shown in Fig. 1 and the characteristic impedances are calculated in these papers. Last year, a paper was published in the IRE TRANS. ON MICROWAVE THEORY AND TECHNIQUE on this problem, using similar methods described below. I wish to describe my approach and show a disparity.

* Received by the PGMTT, December 9, 1958.

¹ H. Kogô and K. Morita, "Electrode capacity of slit-coaxial cylinder," *J. Inst. Elec. Commun. Eng., Japan*, vol. 38, pp. 548-552; July, 1955.

² H. Kogô and K. Morita, "Electrode capacity of slit-coaxial cylinder," (supplement) *J. Inst. Elec. Commun. Eng., Japan*, vol. 39, pp. 33-36; January, 1956.

³ J. Smolarska, "Characteristic impedance of the slotted coaxial line," *IRE TRANS. ON MICROWAVE THEORY AND TECHNIQUE*, vol. MTT-6, pp. 161-164; April, 1958.

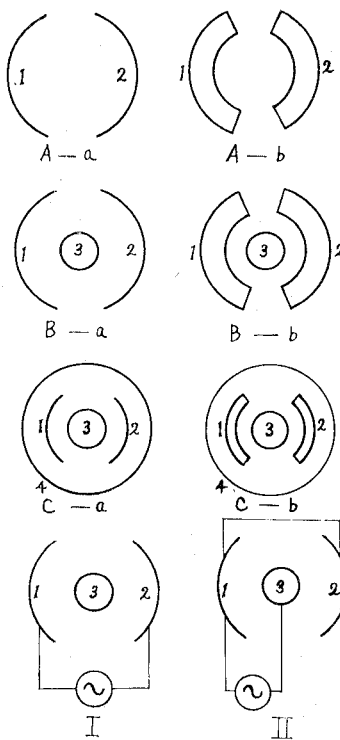


Fig. 1—Cross section of the transmission lines and line construction. A) Split cylinder, B) split coaxial, C) split coaxial with outer pipe; a) thin outer wall, b) thick outer wall; I) line composed of sides 1, 2, II) line composed of sides 1, 2 and central conductor 3.

The characteristic impedance of the split coaxial line shown in Fig. 1 can be classified physically and mathematically as follows:

- A) The split cylinder
 - a) the thin outer wall
 - b) the thick outer wall
- B) The split coaxial line
 - a) the thin outer wall
 - b) the thick outer wall
- C) The split coaxial with outer pipe.

There are two cases. In the first case, the split two sides 1 and 2, compose the transmission line (I) and, in the second case, the split two side 1 and 2, and a central conductor 3 form the transmission line (II) shown in Fig. 1. The mathematical treatment of these cases are difficult because of the thickness of the outer conductors, $A-a$, $A-b$, and $B-a$ in the above table are described in a previous treatise.^{1,2} The same results were obtained by J. Smolarska by using a similar method. For the remaining problems $B-b$, one must rely on an approximate solution, the accurate solution being much too difficult.

The characteristic impedance of $B-b$ with regard to the split coaxial shown in Fig. 2, is acquired from the accurate solution by using the accurate values of the characteristic impedances of the split cylinder considering wall thickness and the split coaxial with thin outer wall.

The characteristic impedance composed of the outer and a central conductor of $B-b$ is almost equal to that compared with the case of a zero thickness since the width of the split is narrow and the disturbance of the split portion shown in Fig. 3 differs slightly by the existence of the thickness.

$$\langle\langle\bullet\bullet\rangle\rangle = \langle\bullet\rangle\langle\bullet\rangle + \langle\bullet\bullet\rangle - \langle\bullet\rangle\langle\bullet\rangle$$

Fig. 2—Relation of the split coaxial line and its composite construction.

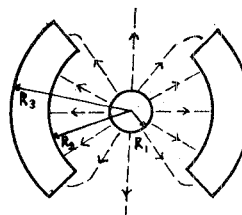


Fig. 3—Disturbance by the thick outer wall.

The curved lines in Fig. 4 show the results of the experiment using a water tank, and these are almost equal to the computed value using the approximate theory. A treatise similar to Smolarska's³ has already been published. Our approach used almost the same transformation equation as found in treatise, but in detail, small differences are found in the papers. For example, Compare A³ with B.¹

- 1) The next formulas are adopted to transform the original figure into the orthogonal line coordinates.
 - A) $\omega = \log Z$ (Transformation).
 - B) $\mu = R_1 e^Z$ (Transformation).
- 2) The $S-C$ transformation is common in both A and B, but the corresponding points differ.
 - A) Corresponds with three unknown constants α , β , and γ for the singular point.
 - B) Corresponds with two unknown constants α , β , for the character of the elliptic function.
- 3) The enumeration method of unknown constants.
 - A) This uses the definite integral, namely a definite integral is used for the distance between each singular point.
 - B) This uses the indefinite integral and substitutes to acquire the value of the corresponding in its consequent equation.
- 4) The numerical computation.
 - A) The numerical computation used the approximate calculating equation as follows: $\beta \gg 1$, $\beta \gg \gamma$, and $\beta \gg \alpha$. These relations are useful only to the case of the particular split angle. However, the errors are not investigated.
 - B) The approximate calculating equation is not in use and accordingly the split width is extended to the whole range.
- 5) The numerical computation of the characteristic impedance is calculated in the following cases.
 - Line I.
 - A) $R/r = 2.3, 2.6, 2.72, 3.37$.
 - B) $Z_0 = 25\Omega, 50\Omega, 150\Omega$, (for the no splits).
 - Line (II).
 - A) $R/r = 2.72$.
 - B) $Z_0 = 25\Omega, 50\Omega, 150\Omega$, (for the no splits).

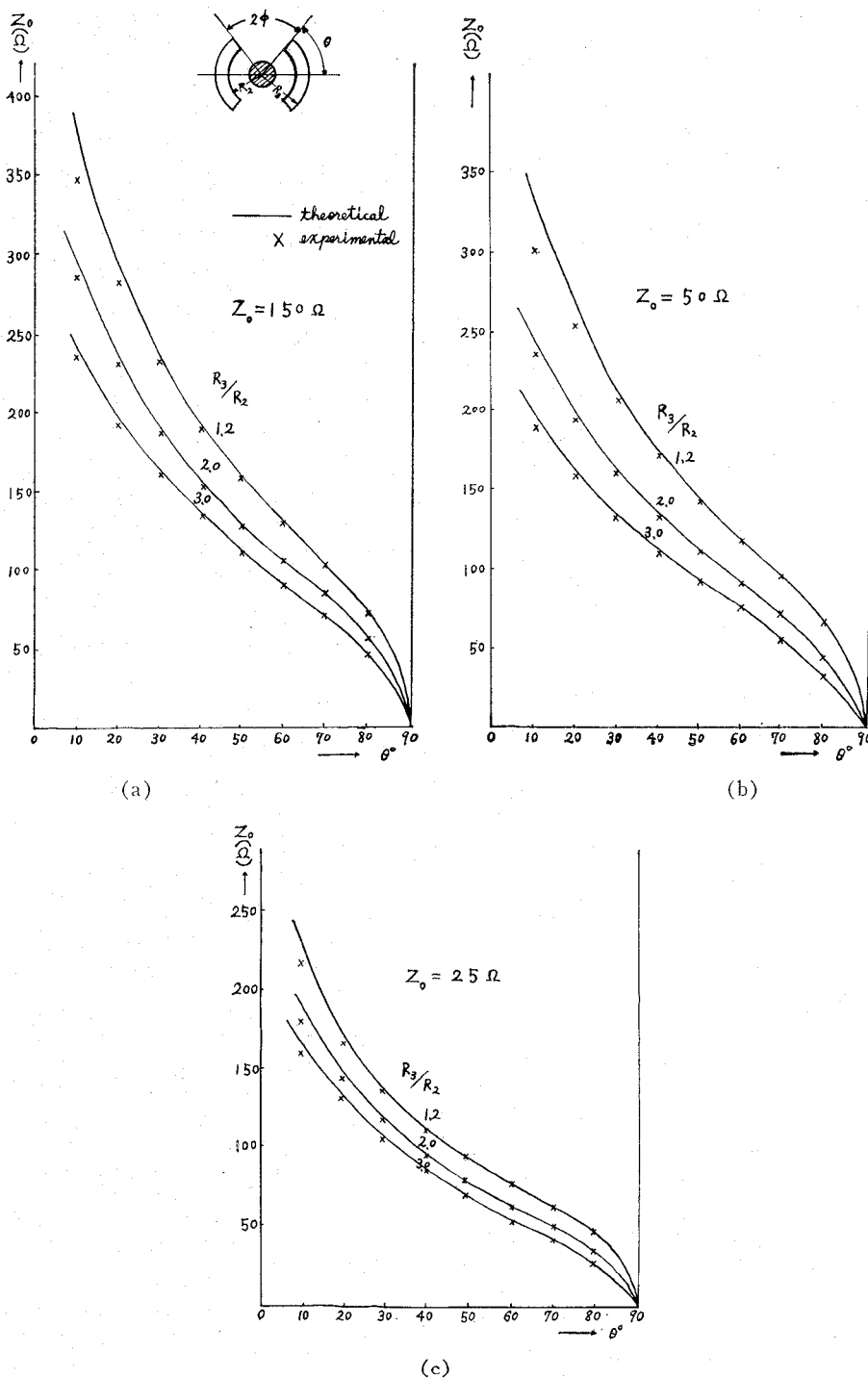


Fig. 4—Characteristic impedance of split coaxial line; (a) case of 150 ohms for the no slit, (b) case of 50 ohms for the no slit, and (c) case of 25 ohms for the no slit.

- 6) The variable range of the split width.
 - A) $2\phi = 10^\circ \sim 40^\circ$.
 - B) the whole range.
- 7) The split coaxial with the thickness of the wall in consideration.
 - A) This is proven⁴ in reference to the split cylinder with the thickness of the wall.

⁴ K. Bochenek, "Impedancia falowa linii wyslepionej wiednym Z rodzajów symetryzatora," *Arch. Electrotech.*, vol. 4, pp. 135-148; April, 1956.

A Method for Enhancing the Performance of Nonreciprocal Microwave Devices*

The performances of nonreciprocal microwave devices are as temperature dependent as the ferrimagnetic materials used to produce them. Hence, the operating characteristics vary markedly with incident power level and ambient temperature. In order to compensate for these temperature changes, special cooling techniques are frequently utilized. Since those are often inconvenient, devices are more usually designed to operate at a much broader frequency range than the specifications demand resulting in deterioration of performance in the specified band. In some cases, ferrites may be especially prepared to have a nearly constant saturation magnetization for a range of temperature, as illustrated in Fig. 1. Whereas both of these ferrites have the same saturation magnetization at room temperature, changing the temperature to 100°C causes a 25 per cent change in the $4\pi M_s$ of the commercially available ferrite, but only a 7 per cent variation in the especially designed one. Tailoring ferrites to the application is much too difficult to represent a solution to the problem.

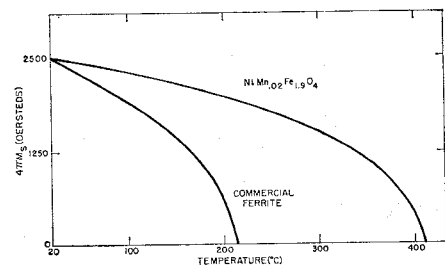


Fig. 1—Saturation magnetization curves for a simple, commercially available ferrite and for an especially designed ferrite having the same $4\pi M_s$ at room temperature.

A simpler solution may be to design devices for operation at the highest ambient temperature to be encountered, or the highest temperature developed because of high input power, and control the temperature of the ferrite to this level. Fig. 2 illustrates one method among many for accomplishing this. Alternatively, some design geometries would lend themselves to an adoption of the well-known technique used in ferromagnetic resonance research: The sample is heated directly through a metal post on which it is mounted in the resonant cavity. A very simple temperature control circuit is required, only regulating to $\pm 10^\circ\text{C}$ or more, since the saturation magnetization does not change very rapidly with temperature even in simple ferrites (Fig. 1). Operation of a nonreciprocal device at a constant elevated temperature results in optimum performance at all power levels and ambient

HIROSHI KOGŌ
Chiba Univ.
531 Iwase
Matsudo, Chiba, Jap.

* Received by the PGMTT, March 18, 1959. This work was done while the author was at the Microwave Physics Lab., Sylvania Elec. Products, Inc., Mountain View, Calif.